DOI: https://doi.org/10.15407/rpra31.01.026
UDC 621.396.96

K. Lukin, D. Tatyanko, O. Zemlyaniy, V. Palamarchuck, M. Zaets
O.Ya. Usikov Institute for Radiophysics and Electronics of the NAS of Ukraine
12, Acad. Proskury St., Kharkiv, 61085, Ukraine
E-mail: lukin.konstantin@gmail.com

DATA ACQUISITION AND MULTITHREAD PROCESSING IN STEPPED-FREQUENCY NOISE GROUND-BASED SAR FOR 2D REAL-TIME IMAGING

Subject and Purpose. *In the paper, the real-time operation of the data acquisition (DAQ) system for stepped-frequency noise ground-based Synthetic Aperture Radar (SAR) is described with an emphasis on DAQ system characteristics and software in an effort to elaborate a real-time operation algorithm on this basis.*

Methods and Methodology. *The real-time operation algorithm outlined in the paper uses Fourier analysis to process input signals acquired with the SAR receiver. The algorithm utilizes multithreading technology to achieve the required real-time performance. The validity of the proposed algorithm is evaluated against conventional signal processing algorithms and techniques using MATLAB packages for numerical analysis and graphic visualization. The experimental investigation of the proposed real-time operation algorithm as part of the software for the developed stepped-frequency noise ground-based SAR was conducted indoors via preliminary laboratory tests.*

Results. *An algorithm for real-time data acquisition and radar imaging has been developed. Its implementation in the software for stepped-frequency noise ground-based SAR enhances the performance of the data acquisition and processing system. A comparative analysis has been performed, showing that the results obtained in the context of the proposed real-time signal-processing program align with reconstructions by standard signal-processing simulation techniques. Measurements performed with the DAQ system as part of the developed stepped-frequency noise ground-based SAR validate our approach and its particular implementation. The observations suggest good target visibility. The target resolution in range and azimuth provided by a 32-element antenna array exceeds that of the 16-antenna configuration. The multithreading approach essentially reduces software runtime. As a result, making a single radar image takes about 10 milliseconds.*

Conclusions. *It has been shown that the developed data acquisition and processing system integrated into stepped-frequency noise ground-based SAR lends itself well to real-time radar imaging.*

Keywords: *stepped-frequency noise ground-based SAR, 2D imaging, data acquisition.*

Introduction

Radar monitoring of moving objects in real time is an important task for many applications [1—9], including traffic monitoring on autobahns and crime deterrence. The matter is highly relevant today, and the Laboratory for Nonlinear Dynamics of Electronic Systems (LNDES) at O.Ya. Usikov IRE NAS of Ukraine pursues thematic studies of various configurations of stepped-frequency ground-based Syn-

Citation: Lukin, K., Tatyanko, D., Zemlyaniy, O., Palamarchuck, V., Zaets, M., 2026. Data acquisition and multithread processing in stepped-frequency noise ground-based SAR for 2D real-time imaging. *Radio Phys. Radio Astron.*, **31**(1), pp. 26—34. https://doi.org/10.15407/rpra31.01.026

thetic Aperture Radar (SAR), with a sharp focus on 2D and 3D real-time imaging [10—14]. In this context, a Ku-band (sub-THz) microwave video camera demonstrator was developed [14].

A current task related to real-time radar measurements is monitoring for moving objects at close range. These measurements have their peculiar features. When an object is moving just a few meters from the radar, it crosses the antenna pattern rather quickly. The narrower the pattern, the faster the crossing. In this case, a critical characteristic of radar is its rapidity of action. The processor speed should be sufficient to track movements and identify individuals.

Surveillance technologies are pertinent in high-traffic areas such as transportation hubs, walkways, and subway stations to detect, for example, weapons concealed under clothing. Security surveillance is essential at checkpoints and entrances. Space is limited there, which favours compact radar systems. To effectively identify a suspect within a two- to five-meter range, the radio image must update every 10 milliseconds (about 100 frames per second). These requirements place quite strict demands on both the hardware and software of a radar. The paper focuses on the data acquisition and processing of radar signals in the developed stepped-frequency SAR.

The DAQ (data acquisition) system hardware is based on 16-channel PCIe-8622 boards from ICP DAS Co., Ltd. (ICP DAS PCIe-8622). Each channel captures an analog signal. Each has an Analog-to-Digital (A/D) converter for Analog-to-Digital Conversion (ADC) of the signal. Thus, the PCIe-8622 board provides a simultaneous measurement of sixteen signals.

The software presents a bottleneck: the radar imaging speed (or frame rate). The remedy is to simplify radar signal processing, giving limited attention to image quality, retaining it within the requirements of radar scene analysis. In the work, this resource is treated in software terms and on the platform of a particular radar device. In addition to simplification benefits, we also gain from splitting the software for radio signal data acquisition and processing into parallel threads. Some samples of the numerical implementation of this radar software and preliminary laboratory tests are presented. To verify the proposed method and its numerical implementation, comparisons are provided with MATLAB-based modeling and processing of radar return signals from different observation points.

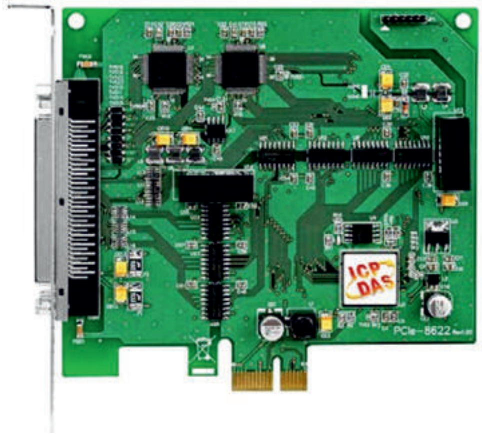

Fig. 1. The DAQ board ICP DAS PCIe-8622

The algorithm for two-dimensional (2D) imaging based on the developed stepped-frequency noise ground-based SAR (hereinafter, the SAR) is developed in the context of harmonic waveforms.

1. Data Acquisition System Design

The Data Acquisition (DAQ) system of the SAR is based on the ICP DAS PCIe-8622 DAQ board that supports the PCI Express bus. The DAQ board has 16 channels, each with a 16-bit A/D converter. This design allows simultaneous and parallel sampling of input signals. Each channel features a programmable input range of ±10 V or ±5 V with a sampling rate up to 200 kilosamples per second. The appearance of the DAQ board ICP DAS PCIe-8622 is shown in Fig. 1 [15, 16].

Cascading four 16-channel DAQ boards makes a 64-channel DAQ radar device. The block diagram of the developed synchronous 64-channel 16-bit ADC DAQ system is shown in Fig. 2.

Signals picked up by the receiving antenna array (not shown) and routed through the quadrature detectors are directed to the DAQ system, as illustrated in Fig. 2. Overall, 32 In-phase (IP) and 32 Quadrature (Q) signals are fed into the DAQ system. The four 16-channel DAQ boards, ICP DAS PCIe-8622, capture 64 signals from the quadrature detectors.

When an external control signal is applied to the external trigger inputs, the sixty-four ADC channels of the four DAQ boards simultaneously record signals from the quadrature detectors. The next step

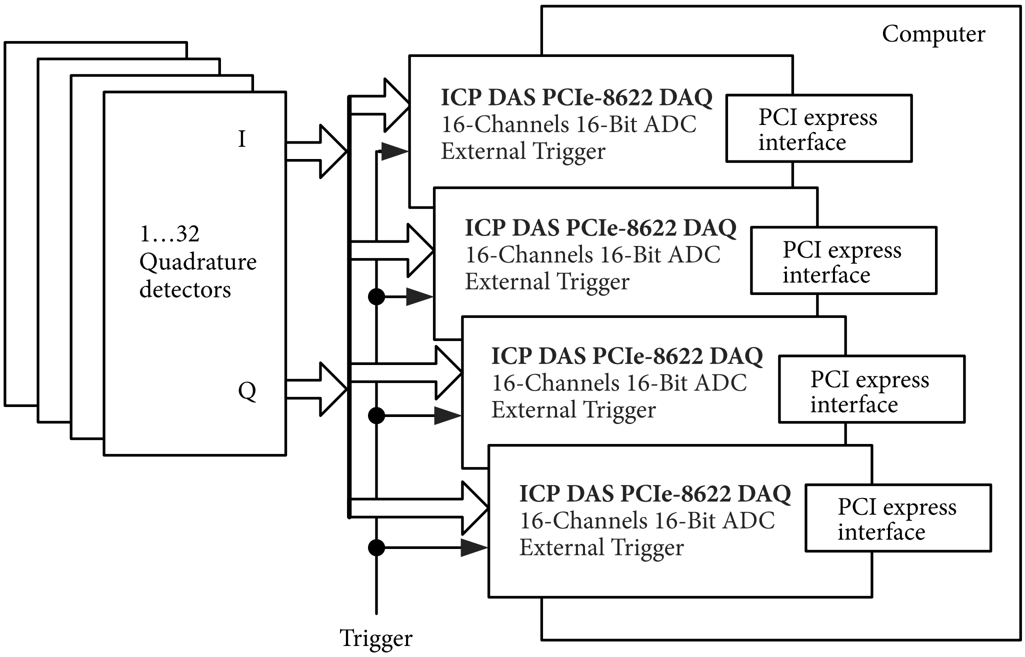

Fig. 2. Block diagram of the 64-channel 16-bit ADC DAQ system

is to direct the resulting data to the computer for further processing.

2. Algorithm for Data Processing and SAR Imaging

An algorithm was constructed to operate the stepped-frequency noise ground-based SAR developed for 2D real-time radar imaging. The data extracted from the SAR receiver are processed to yield 2D real-time images. The principal points in the algorithm development are reported below.

1) The 2D real-time radio imaging algorithm is valid in the context of harmonic waveforms. The results of the A/D conversion of input signals of the DAQ boards make a 2D array (Fig. 3, *a*) of complex numbers. In this case, the IP signals are assigned to the real part of the number array, and the Q signals from the quadrature detector output of each antenna channel produce the imaginary part of this number array. In our program, the number array is structured such that each column contains all samples (frequency scans) for every antenna channel. In toto, the number array has 64 columns for the antenna's 64 channels. And each channel includes a set of signal measurements at the quadrature detector output at all the frequencies (at a given number of frequency steps).

2) The formed number array provides us with the initial data for deriving the range profile (Fig. 3, *b*) via the Inverse Fourier Transform (IFT). The IFT program code is written upon the Inverse Discrete Fourier Transform (IDFT), $s(k)$, [17] in the form

$$s(k) = \\ = \frac{1}{N}\sum_{n=0}^{N-1} S(n)(\cos(2\pi kn / N) + j\sin(2\pi kn / N)), \quad (1)$$

where n and k are the sample indices in the time and spectral series, respectively, N is the total number of the time series terms, and $S(n)$ is the signal level of the n-th sample.

The IFT of the data taken at the outputs of the quadrature detectors yields the range profile array for all antenna channels. In our program, the columns of the resulting number array produce range profiles for each antenna channel.

3) The row-wise Fourier transform of the range-profile array yields the azimuth compression (Fig. 3, *c*).

4) Further, optionally (at the user's choice), the data are presented logarithmically, by taking a decimal logarithm from each element of the resulting array as follows

$$a_{n\_\log 10} = \log_{10}(a_n), \quad (2)$$

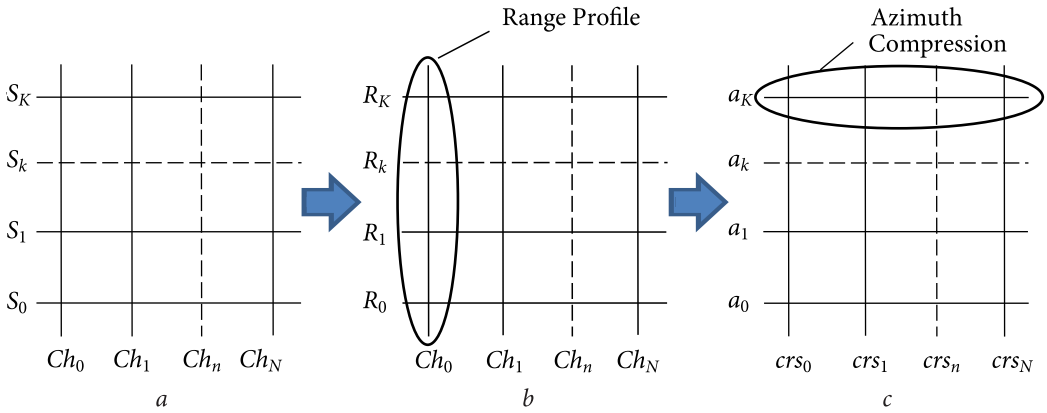

Fig. 3. Real-time data-flow processing in the SAR receiver for 2D imaging: (*a*) format of the data array after the A/D conversion: Ch_n is the n-th channel of the antenna array, S_k is the k-th sample (measured at the ADC output), and K is the total number of samples; (*b*) array of range profiles: R_k is the k-th element in the range-profile array for the corresponding antenna-array channel and K is the total number of these elements; (*c*) azimuth compression array: crs_n is the n-th cross-range sample, a_k is the k-th element in the azimuth compression array, and K is the total number of these elements

where a_n is the n-th element of the azimuth compression array.

5) Next, the maximum-value element of the array is determined. The resulting image is normalized to that level by reducing all array elements to the form

$$a_{i\_norm} = a_i \,/\, a_{\max}, \qquad (3)$$

where a_i is the i-th element of the azimuth array, a_{i_norm} is the i-th element of the normalized azimuth array, and $a_{\max}$ is the maximum-value element in the azimuth array.

6) Formation of the stepped-frequency noise ground-based SAR image and the image display on the monitor.

The software colors and displays a color table from blue (lower) to red (upper).

The resulting azimuth-compression array is converted to the BMP format using the color table and is displayed on the monitor.

3. SAR Receiver Software and Its Implementation

The multithreading program developed for the receiver of stepped-frequency ground-based noise SAR uses Microsoft Visual C++ 2015 and Windows Forms.

The developed software operates four ICP DAS PCIe-8622 DAQ boards. It consists of a load unit that provides functionality for the DAQ board operation (data acquisition and preprocessing) and a main module. The main module manages general data processing, radar ima-ging, and image display.

One of the primary functions of the SAR receiver is to display radar images in real time. To reduce the time of radar signal measurement, the program is divided into asynchronous threads. Each data acquisition (DAQ) board operates within its own thread, allowing different parts of the program to run in parallel. This approach enables each DAQ board to acquire data individually and simultaneously with the others, significantly decreasing the time needed for signal measurement and data processing.

Four threads are used to acquire I/Q signals from the DAQ boards. The fifth (main) thread is responsible for data processing and display.

The key modules of the multithreading program of the SAR receiver are:

Threads #1—4, produce A/D conversion of 16 input signals by DAQ boards #1—4, and

Thread #5 (the main thread of processing and display) produces:

1) conversion of ADC output data to a format suitable for further processing,

2) range profile calculation for each ADC channel,

3) azimuth calculation from the range profile,

4) signal waveform display of one selected ADC channel,

5) range profile display of one selected ADC channel,

6) radio imaging and display.

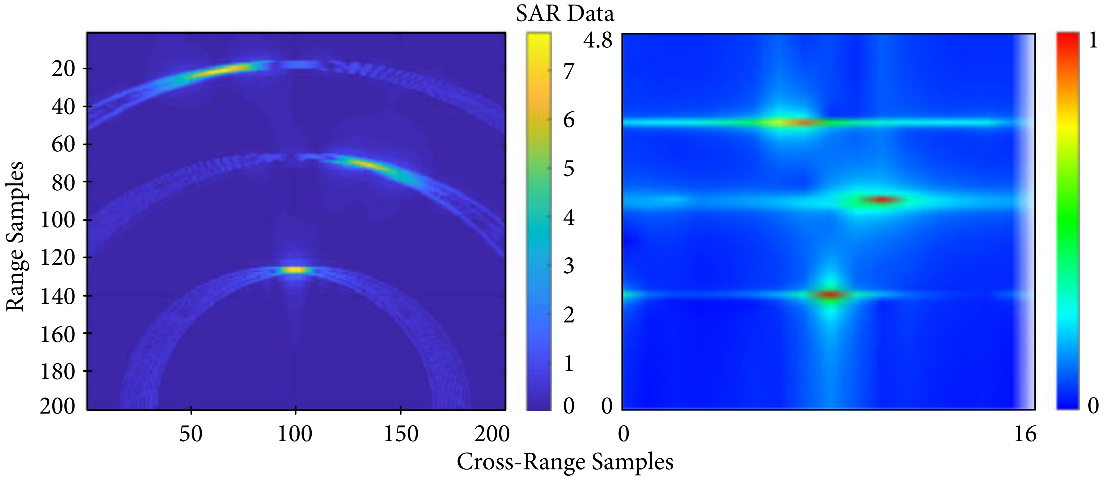

a *b*

Fig. 4. Three-target configuration: (*a*) the image simulated by established methods in MATLAB and (*b*) the radar image generated by the designed SAR receiver program incorporating the proposed streamlined processing algorithm. Here $D_1 = 2.6$ m, $\alpha_1 = 15.6°$, $D_2 = 1.4$ m, $\alpha_2 = 0°$, and $D_3 = 3.6$ m, $\alpha_3 = -11.3°$

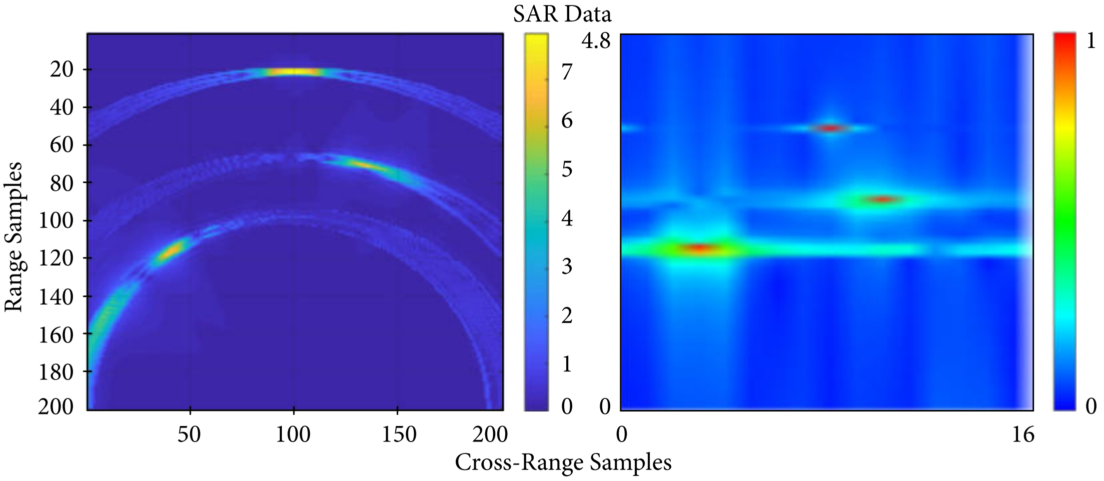

a *b*

Fig. 5. Three-target configuration: (*a*) the image simulated by established methods in MATLAB and (*b*) the radar image generated by the designed SAR receiver program incorporating the proposed streamlined processing algorithm. Here, $D_1 = 2.6$ m, $\alpha_1 = 15.6°$, $D_2 = 1.4$ m, $\alpha_2 = -45°$, and $D_3 = 3.5$ m, $\alpha_3 = 0°$

The SAR receiver software works as follows. The DAQ boards are awaiting an external synchronizing trigger signal. It simultaneously starts the A/D conversion by the four 16-channel DAQ boards, with the number of A/D conversions equal to the number of frequency steps. After completing the A/D conversion, the next trigger signal is waited for. This code is implemented by four identical program threads #1—4, one for each DAQ board.

Thread #5 contains a code for digital processing and display of the acquired data, including range profile calculation for each SAR receiver channel, azimuth calculation, radar imaging, and display.

The data processing and display within Thread #5 use a software timer interrupt. It smoothing the time interval between different image displays. To this end, we adopt a standard Visual C++ and Windows Forms Timer with a 1 ms interval.

Thus, all Threads #1—5 operate simultaneously, in parallel, and asynchronously. Threads #1—4 assigned to the DAQ boards run the A/D conversion of input signals and preprocess the data for further processing. After the A/D conversion, the data from Threads #1—4 are sent to Thread #5 for further processing and display.

4. Estimation of Two-Threaded Program Runtime

The thread technology significantly streamlines the program. The total runtime of the program depends mostly on the number of samples collected per measurement, which corresponds to the number of signal frequency steps. The time of DAQ board sampling is almost constant and hardly depends on the number of samples, whereas the time for data processing and display does. Another expedient that assists in speeding up the sampling is the Direct Memory Access (DMA) method. The DMA method for DAQ boards speeds up sampling by approximately 1.5 times. The Table below shows sampling, processing, and display runtimes for various sample numbers, with and without threading.

The experimental conditions are: 16 channels, 100—1000 samples (100—1000 frequency steps), and a sampling rate of 200 kilosamples per second. The DMA mode method is adopted.

The fewer the samples, the greater the benefits from the program's multithreading.

Thus, the Table shows that threads significantly streamline the program execution.

5. Simulation of Data Processing in Stepped-Frequency SAR

To evaluate the performance of the signal-processing algorithm within the developed SAR program, return signals from objects were manipulated in different contexts. The simulated radar scenes contained various sets of objects. The modeled return signals were processed by established MATLAB methods [18] to compare their results with those produced by the proposed algorithms integrated into the developed program for stepped-frequency noise ground-based SAR.

Let us take a set of three pointwise scatterers. The operating frequency range spans 12 to 16 GHz. The antenna array has 16 elements. The number of frequency samples is 128. The antenna array is such that the horizontal spacing between the antenna elements is 9.4 mm, and the vertical offset between the symmetry centers of even- and odd-numbered elements is 45 mm.

The objects in the scene and the even-numbered antenna-array elements are mounted at the same height, while the odd-numbered antenna-array elements are placed 45 mm higher. The distance between the scatterer and the antenna-array center of symmetry is D_i. The angle between the direction to the object and a perpendicular to the antenna-array center of symmetry is α_i. The positive angle value corresponds to the right side of the SAR image.

Figures 4, *a* and 5, *a* display images generated by established methods in the MATLAB environment [18, 19]. Examples of images generated by the designed SAR receiver program incorporating the proposed streamlined processing algorithm are illustrated in Figs 4, *b* and 5, *b*. The target coordinates are given in the captions.

Comparing the results with MATLAB and those produced by the developed program shows their agreement on both sizes and mutual arrangements of the scatterers. Yet, the radar image generation with MATLAB took tens of seconds (about 20 s), while the same task using our radar program took only tens of milliseconds (see the Table). This makes the proposed signal-processing algorithm favorable and capable of producing real-time radar movies within the developed radar program.

6. Experimental Tests of Stepped-Frequency Noise Ground-Based SAR

The LNDES team conducted indoor measurements of frequency-stepped noise ground-based SAR under the following laboratory conditions:

- generator settings: upper frequency 16 GHz, lower frequency 12 GHz, and the number of frequency steps 128;
- SAR receiver settings: ADC sampling rate 5000 samples per second and configurations of 16 and 32 Vivaldi antennas (32 and 64 ADC channels, respectively).

Comparison of SAR program versions

Samples per measurement	Maximum measurement time, ms		Time saving, ms	Time saving, %
	without threads	with threads		
1000	95	80	15	15.8
100	19	11	8	42.1

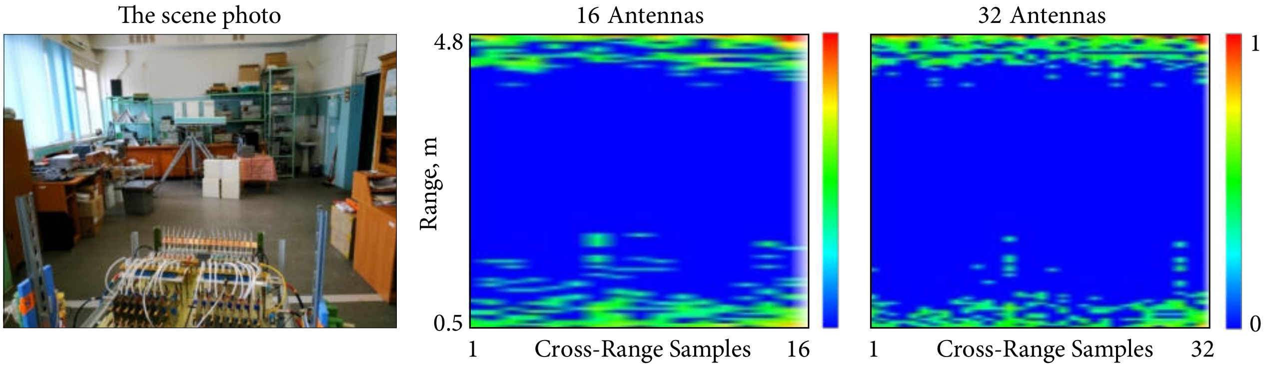

a *b* *c*

Fig. 6. The scene without targets: the picture (*a*) and radar images using 16- and 32-element antennas (*b* and *c*, respectively)

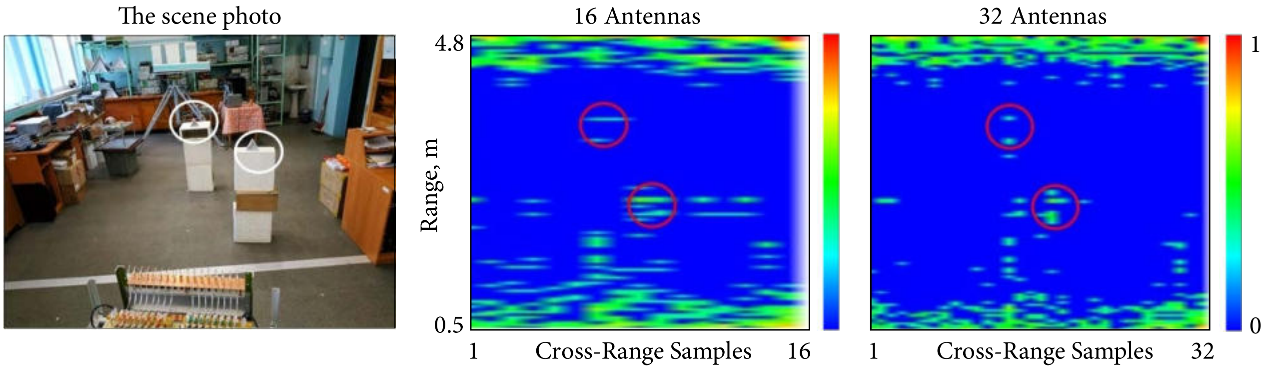

a *b* *c*

Fig. 7. Two corner reflectors: the picture (*a*) of the measurement scene and radar images using 16- and 32-element antennas (*b* and *c*, respectively)

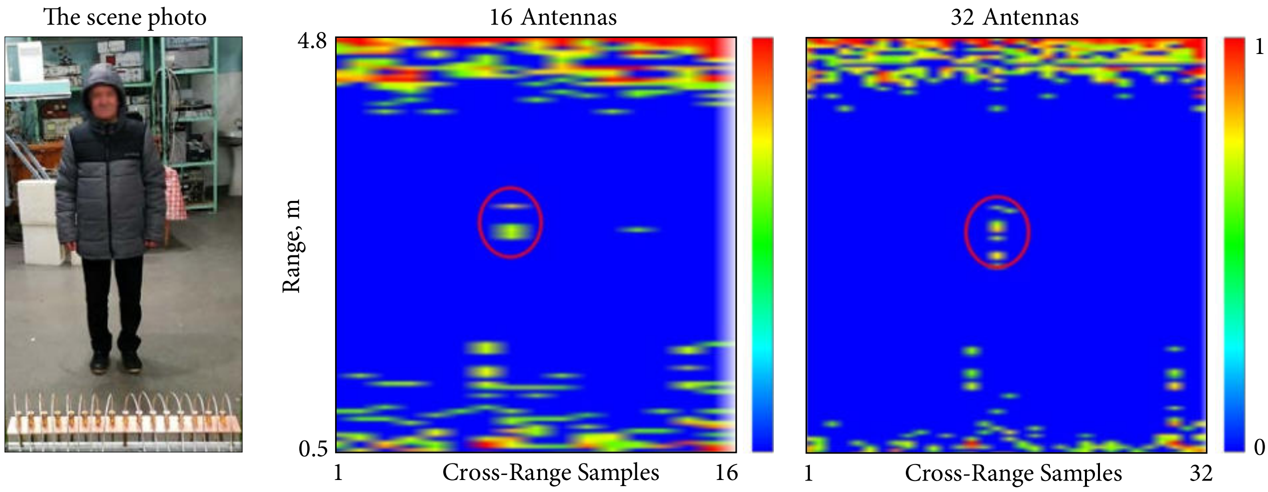

a *b* *c*

Fig. 8. A man in front of the radar: a picture (*a*) of the scene and radar images using 16- and 32-element antennas (*b* and *c*, respectively)

The measurement scene was indoors, in a laboratory room. The scatterers were two corner reflectors, an AK-47 assault rifle, a handgun, and a man (during one of the measurements). The measurements were made using 16- and 32-element Vivaldi antenna arrays to compare the radar image resolutions.

The measurement scene without targets is shown in Fig. 6. Only wave reflections from walls, furniture, and laboratory equipment are observed.

The scene with two corner reflectors as targets is illustrated in Fig. 7. The ranges of the left and right corners are 2.9 and 1.7 m, respectively, and the azimuth spacing between the corners is 0.4 m.

The scene in Fig. 8 has a man in front of the radar.

Although the experiments were conducted in a laboratory rather than in an anechoic chamber, the environment resembled real radar operating conditions. Understandably, the radar image contains re-reflections from walls, equipment, and furniture. Nevertheless, the useful signal was successfully extracted, and the target, even in motion, was identified. The measurement results indicate improved target visibility. The range and azimuth resolutions provided by a 32-antenna radar are superior to those of a 16-antenna radar.

Conclusions

An algorithm for data acquisition and real-time radar imaging has been designed, implemented in the software for stepped-frequency noise ground-based SAR, and verified numerically against established radar image simulation methods and experimentally in the context of preliminary laboratory tests.

It has been shown that the developed data acquisition and processing system as part of the stepped-frequency noise ground-based SAR lends itself well to real-time radar imaging. The real-time functionality was achieved by dividing the radar program into multiple threads, each running in parallel and performing its own specific task. This use of multithreading significantly reduces the software runtime. The time taken for a single radar image is approximately 10 ms. With this processing speed, the system can effectively track target movement in real time. The use of 64-channel A/D converters in a 32-antenna radar configuration substantially improves radar image resolution compared with 32-channel A/D converters in a 16-antenna configuration.

The work has been carried out in the Laboratory for Nonlinear Dynamics of Electronic Systems (LNDES) at the O.Ya. Usikov Institute for Radiophysics and Electronics of the National Academy of Sciences of Ukraine (IRE NASU) under the NATO project G5395 SPS.

REFERENCES

1. Batool, S., Frezza, F., Mangini, F., Simeoni, P., 2020. Introduction to Radar Scattering Application in Remote Sensing and Diagnostics: Review. *Atmosphere*, **11**(5), 517. DOI: 10.3390/atmos11050517
2. Moreira, A., Prats-Iraola, P., Younis, M., Krieger, G., Hajnsek, I., Papathanassiou, K.P., 2013. A tutorial on synthetic aperture radar. *IEEE Geosci. Remote Sens. Mag.*, **1**(1), pp. 6—43. DOI: 10.1109/MGRS.2013.2248301
3. Park, S., Kim, Y, Lee, K., Smith, A.H., Dietz, J.E., Matson, E.T., 2020. Accessible Real-Time Surveillance Radar System for Object Detection. *Sensors*, **20**(8), 18 pp. DOI: 10.3390/s20082215
4. Cumming, I.G., Wong, F.H., 2005. *Digital Processing of Synthetic Aperture Radar Data: Algorithms and Implementation.* Norwood, MA: Artech House.
5. Woodhouse, I., 2006. *Introduction to Microwave Remote Sensing*. Boca Raton, FL: CRC Press.
6. Oliver, C., Quegan, S., 2004. *Understanding Synthetic Aperture Radar Images*. Herndon, VA: SciTech Publishing.
7. Tomiyasu, K., 1978. Tutorial review of synthetic-aperture radar (SAR) with applications to imaging of the ocean surface. *Proc. IEEE,* **66**(5), pp. 563—583. DOI: 10.1109/PROC.1978.10961
8. Henderson, F., Lewis, A., 1998. *Manual of Remote Sensing: Principles and Applications of Imaging Radar*. New York: Wiley.
9. Curlander, J.C., McDonough, R. N., 1991. *Synthetic Aperture Radar: Systems and Signal Processing*. New York: Wiley.
10. Lukin, K.A., 2001. Noise Radar Technology. *Telecommunications and Radio Engineering*, **55**(12), pp. 8—16.
11. Vyplavin, P., Melnikova, E., Lukin, S., 2010. Real-time signal processing in noise radar. In: *Proc. 11th Int. Radar Symposium (IRS-2010).* Vilnius, Lithuania, 16—18 June 2010, pp. 1–3.
12. Lukin, K.A., Moreira, J.R., Vyplavin, P.L., Lukin, S.K., Zemlyaniy, O.V., 2013. FPGA based software defined noise radar. *Appl. Radio Electron.*, **12**(1), pp. 89—94.
13. Lukin, S., Zemlyaniy, O., Palamarchuk, V., Tatyanko, D., Lukin, K., Pascazio, V., *2018.* Methods for Generation of Probing Signals in Software Defined Noise Radar. In: *Proc. 2018. 19th Int. Radar Symp. (IRS).* Bonn, 2018, pp. 1—9. DOI: 10.23919/IRS.2018.8448097
14. Lukin, K., Palamarchuk, V., Zemlyanyi, O., Tatyanko, D., Zaets, N., Shelekhov, O., Lukin, S., Jarabo Amores, P., and Rosa Zurera, M., 2023. Ku-Band (sub-THz) Demonstrator of Microwave Video Camera. *URSI Radio Sci. Lett.,* **4**, pp. 59—63. DOI: 10.46620/22-0059

15. ICP DAS CO., LTD, 2024. PCIe-8622 ICP DAS Data Sheet [pdf]. Available at: https://www.icpdas.com/web/product/download/pc_boards/document/data_sheet/PCIe-8622_en.pdf
16. ICP DAS CO., LTD, 2015. PCIe-862x Series User Manual [pdf]. Available at: https://www.icpdas.com/web/product/download/pc_boards/document/manual/pcie-862x_user_User_Manual_v10_en.pdf
17. Lyons, R.G., 2011. *Understanding Digital Signal Processing*. 3rd ed. Prentice Hall. Upper Saddle River, NJ.
18. Soumekh, M., 1999. *Synthetic Aperture Radar Signal Processing: with MATLAB Algorithms*. State University of New York, Buffalo, John Wiley & Sons, Inc., ISBN: 0-471-29706-2.
19. MATLAB SAR Toolbox. Available at: https://github.com/ngageoint/MATLAB_SAR

Received 20.02.2025

К.О. Лукін, Д.М. Татьянко, О.В. Земляний, В.П. Паламарчук, М.К. Заєць
Інститут радіофізики та електроніки ім. О.Я. Усикова НАН України
вул. Акад. Проскури, 12, м. Харків, 61085, Україна

ЗБІР ДАНИХ ТА БАГАТОПОТОКОВА ОБРОБКА В ШУМОВОМУ НАЗЕМНОМУ РСА ЗІ СТУПІНЧАСТОЮ ЗМІНОЮ ЧАСТОТИ ДЛЯ ОТРИМАННЯ 2D-ЗОБРАЖЕНЬ У РЕАЛЬНОМУ ЧАСІ

Предмет і мета роботи. У статті описано систему збору даних для шумового наземного РСА зі ступінчастою зміною частоти, яка працює в режимі реального часу. Описано її характеристики та програмне забезпечення з акцентом на розробку алгоритму роботи в реальному часі.

Методи та методологія. Описано алгоритм роботи в режимі реального часу, що заснований на фур'є-аналізі сигналу з приймача шумового наземного РСА зі ступінчастою зміною частоти та інтегрований у програмне забезпечення цього РСА. Для забезпечення роботи приймача РСА в режимі реального часу в програмному забезпечені, що розроблене на основі запропонованого алгоритму, застосовано технологію багатопотоковості. Коректність роботи запропонованого алгоритму перевірено за допомогою традиційних алгоритмів та методів обробки сигналів, які були реалізовані із застосуванням пакету прикладних програм для чисельного аналізу MATLAB. Роботу запропонованого алгоритму було експериментально досліджено в лабораторних умовах у складі програмного забезпечення шумового наземного РСА зі ступінчастою зміною частоти, що був розроблений.

Результати. Розроблено алгоритм збору даних та радіолокаційної візуалізації в реальному часі, реалізований у програмному забезпеченні для шумового наземного РСА зі ступінчастою зміною частоти. Роботу алгоритму перевірено чисельно за допомогою відомих методів моделювання радіолокаційних зображень, а також експериментально в лабораторних умовах. Порівняльний аналіз показав збіг результатів обробки сигналів програмою в реальному часі та результатів, отриманих при моделюванні обробки сигналів загальноприйнятими методами. Результати вимірювань за допомогою цієї системи у складі розробленого авторами шумового наземного РСА зі ступінчастою зміною частоти показали хорошу видимість цілей і покращення роздільної здатності цілей за дальністю та азимутом при використанні конфігурації з 32 антенами порівняно з конфігурацією з 16 антенами. Завдяки застосуванню потокової технології значно скоротився час виконання програми, що дозволило забезпечити час отримання одного радіолокаційного зображення близько 10 мс.

Висновки. Показано, що розроблена система збору та обробки даних у складі шумового наземного РСА зі ступінчастою зміною частоти дозволяє формувати радіолокаційні зображення в режимі реального часу.

Ключові слова: *шумовий наземний РСА зі ступінчастою зміною частоти, 2D-зображення, збір даних.*